DOI: 10.1002/anie.201005869

Bioinorganic Chemistry

An Oxocobalt(IV) Complex Stabilized by Lewis Acid Interactions with Scandium(III) Ions[**]

Florian Felix Pfaff, Subrata Kundu, Marcel Risch, Shanthi Pandian, Florian Heims, Iweta Pryjomska-Ray, Peter Haack, Ramona Metzinger, Eckhard Bill, Holger Dau, Peter Comba, and Kallol Ray[*]

Dedicated to Professor Karl Wieghardt on the occasion of his retirement

Terminal $\{Co^{IV}{-}O\}$ complexes have been proposed as reactive intermediates in a number of cobalt-mediated alkane hydroxylation reactions[1] and in the catalytic four-electron reduction of dioxygen to water.[2] However, direct spectroscopic characterization of Co^{IV}-containing species in these systems has not been reported, leaving a definitive assignment ambiguous. Evidence of the presence of terminal $\{Co^{IV}{-}O\}$ units is to date limited to mass spectrometric studies in the gas phase.[3] Reports of oxo-bridged Co^{IV}-containing units, which are proposed as key intermediates in the catalytic oxidation of water to give molecular oxygen,[4] are also extremely rare.[5] Efforts to model $\{Co^{IV}{-}O\}$ intermediates have most likely been hampered by the anticipated large $Co^{III/IV}$ oxidation potential,[5a,b] and strong electron repulsion between the electron rich oxo- and cobalt centers.[6]

Herein we present the synthesis of a terminal $\{Co^{IV}{-}O\}$ complex stabilized by the tetradentate tripodal ligand TMG_3tren (tris[2-(*N*-tetramethylguanidyl)ethyl]amine),[7] which has recently found application in the successful stabilization of superoxocopper(II)[8] and high-spin ($S = 2$) $\{Fe^{IV}{=}O\}$[9] complexes. This ligand is expected to enforce a trigonal bipyramidal (TBP) geometry at the Co^{IV} center that is present in the isoelectronic $\{Fe^{III}{-}O\}$ complex of the tris(ureaylato) ligand employed by Borovik and co-workers.[10] However, the TMG_3tren ligand lacks the hydrogen-bonding groups of the tris(ureaylato) ligand that were necessary to stabilize the $\{Fe^{III}{-}O\}$ unit.[10] In our case, the stabilization of the $\{Co^{IV}{-}O\}$ group is achieved by utilizing its Lewis acid interaction with Sc^{3+} ion, thereby forming a $\{Co^{IV}{-}O{-}Sc\}^{3+}$ unit. A similar interaction between a high-valent oxomanganese center and Ca^{2+} in the oxygen-evolving complex of photosystem II has been proposed to play a vital role in oxygen evolution during photosynthesis.[11] Binding of the redox inactive Ca^{2+} and Sc^{3+} ions to the non-heme oxoiron(IV) complex $[(TMC)Fe^{IV}(O)]^{2+}$ (TMC = 1,4,8,11-tetramethyl-1,4,8,11-tetraazacyclotetradecane) has also been recently reported to significantly affect its redox properties.[12]

Reaction of equimolar amounts of TMG_3tren and $Co^{II}(OTf)_2$ in CH_2Cl_2 afforded $[Co^{II}(TMG_3tren)(OTf)](OTf)$ (**1**-OTf); the crystal structure (Scheme 1) exhibits the expected TBP geometry ($\tau^{[13]} = 0.97$). Reaction of **1**-OTf in CH_2Cl_2 with three equivalents of 2-(*tert*-butylsulfonyl)iodosylbenzene ($^{s}PhIO$)[14] at −60 °C for two hours generated an orange complex **2** with absorption maxima $\lambda_{max}(\varepsilon_{max})$ centered at 520(250) and 722(100) nm (Figure 1, dotted line). Interestingly, when the above reaction was performed in presence of one equivalent of $Sc(OTf)_3$, a new species **3** was formed with absorption maxima $\lambda_{max}(\varepsilon_{max})$ centered at 489(495) and 810(100) nm (Figure 1, dashed line). Complex **3** could also be obtained by reacting **1** with $^{s}PhIO$ in the presence of 2-(*tert*-butylsulfonyl)iodobenzenediacetate ($^{s}PhI(OAc)_2$).[14,15]

Compounds **2** and **3** were unstable at 25 °C, with half-lives ($t_{1/2}$) of 20 and 120 seconds, respectively. Whereas **2** decayed to a green species with $\lambda_{max}(\varepsilon_{max})$ centered at 690(300) nm, **3** decayed to a yellowish-green species with no characteristic feature in the UV/Vis spectrum (Supporting Information, Figure S1). We have not yet determined the identity of the metal-containing species that results from these decay processes.

The electrospray mass spectrum of **3** (Figure 1 inset; Supporting Information, Figure S2) has signals at $m/z = 664.3$ and 257.2, with isotope distribution patterns consistent with their respective formulation as $\{[Co^{IV}(O)(TMG_3tren)](OTf)\}^{+}$ and $[Co^{IV}(O)(TMG_3tren)]^{2+}$. ^{18}O labeling of **3** caused the peaks to shift to $m/z = 666.3$ and 258.2, respectively. In contrast, spectra of **2** displayed an intense peak at $m/z = 663.3$ (Figure 1 inset; Supporting Information, Figure S3), suggesting the formation of a species that is one

---

[*] F. F. Pfaff, S. Kundu, F. Heims, Dr. I. Pryjomska-Ray, P. Haack, R. Metzinger, Dr. K. Ray
Humboldt-Universität zu Berlin, Institut für Chemie
Brook Taylor Strasse 2, 12489 Berlin (Germany)
Fax: (+49) 302-093-6966
E-mail: kallol.ray@chemie.hu-berlin.de
M. Risch, Prof. Dr. H. Dau
Freie Universität Berlin, FB Physik
Arnimallee 14, 14195 Berlin (Germany)
Dr. S. Pandian, Prof. Dr. P. Comba
Anorganisch-Chemisches Institut der Universität Heidelberg
Im Neuenheimer Feld 270, 69120 Heidelberg (Germany)
Dr. E. Bill
Max-Planck-Institut für Bioanorganische Chemie
Stiftstrasse 34–36, 45470 Mülheim an der Ruhr (Germany)

[**] We gratefully acknowledge financial support of this work from the Cluster of Excellence "Unifying Concepts in Catalysis" (EXC 314/1), Berlin. We thank F. Schäfers and M. Mertin (beamline KMC-1, BESSY, Berlin) for technical support. We are also grateful to Prof. P. Hildebrandt, Prof. C. Limberg, and Dr. U. Kuhlmann for helpful discussions.

Supporting information for this article is available on the WWW under http://dx.doi.org/10.1002/anie.201005869.

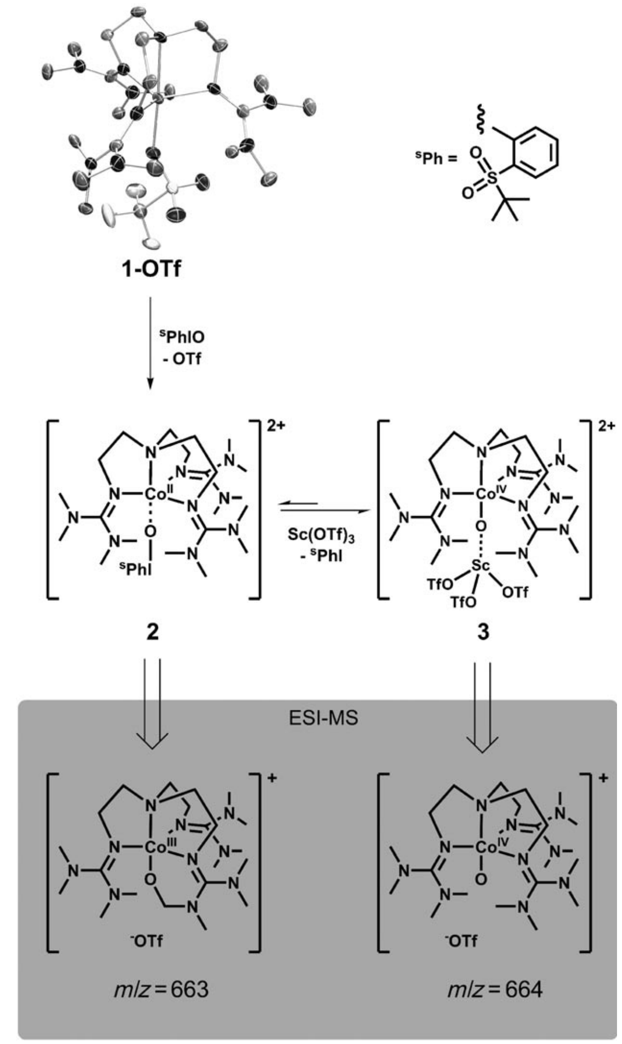

Scheme 1. The formation of **2** and **3** from **1**-OTf. The decay of **2** and **3** under the conditions of ESI-MS is shown in the shaded region. $TfO^- = CF_3SO_3^-$.

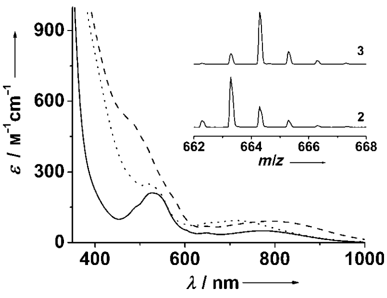

Figure 1. Electronic spectra of **1**-OTf (——), **2** (•••••), and **3** (-----) in CH_2Cl_2 at −60 °C. Inset: Electrospray mass spectra of **2** and **3** in CH_2Cl_2.

hydrogen atom lighter than **3**. From simulation of the observed isotope distribution patterns, the peak at $m/z = 663.3$ is formulated as $\{[Co^{III}(O)(TMG_3trenH)](OTf)\}^+$ and derives from the alkoxocobalt(III) product (Scheme 1), resulting from self-hydroxylation of the ligand. ^{18}O labeling of **2** also caused the product-derived peak to shift to $m/z = 665.4$ with isotopic distribution patterns consistent with a high percentage of ^{18}O incorporation into the products. The electrospray mass spectra of **2** and **3** thus suggest a possible role of Sc^{3+} in stabilizing the highly reactive $\{Co^{IV}(O)\}^{2+}$ unit in **3**. In absence of Sc^{3+} decay of the $\{Co^{IV}(O)\}^{2+}$ unit occurs under the conditions of the electrospray mass measurements possibly by a self-hydroxylation process, thereby yielding an alkoxocobalt(III) product (Scheme 1).

The electronic structures of the cobalt complexes **1**–**3** were investigated by EPR spectroscopy. The EPR spectrum of **1**-OTf has axial symmetry, with effective g values of $g_{\perp}^{\text{eff}} = 4.60$ and $g_{\parallel}^{\text{eff}} = 2.10$, thereby indicating an $S = 3/2$ ground state (Figure 2). A weak resonance feature is also observed at $g^{\text{eff}} = 6$, which indicates a large Boltzmann population of the "$m_s = \pm 3/2$" levels owing to negative zero-field splitting.[16] The experimental spectrum of **1**-OTf was simulated with g values of $g_{\perp} = 2.23$ and $g_{\parallel} = 2.09$, vanishing rhombicity, $E/D \approx 0$, and a negative D value of $(-10 \pm 2)\ \text{cm}^{-1}$. A characteristic eight-line ^{59}Co hyperfine pattern is observed at g^{eff}_z (Figure 2) according to an A_z component of the hyperfine coupling

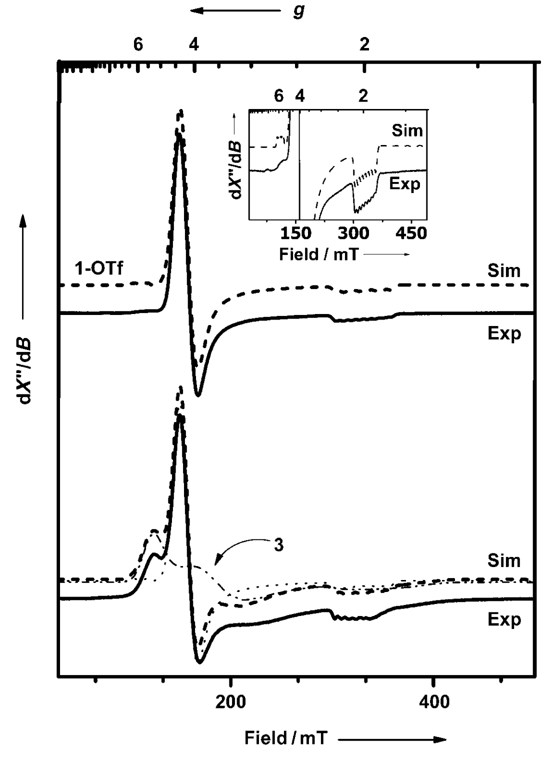

Figure 2. X-Band EPR spectra. Top: Spectrum of **1**-OTf in CH_2Cl_2 at 10 K (frequency 9.63191 GHz; power 0.20 mW; modulation 0.75 mT; simulation parameters: $D = (-10 \pm 2)\ \text{cm}^{-1}$, $E/D = 0.02$, $\sigma(E/D) = 0.02$, $g_x = 2.23$, $g_y = 2.23$, $g_z = 2.09$, $A_z = 75 \times 10^{-4}\ \text{cm}^{-1}$). Expansion of the $g = 2$ and $g = 6$ regions are shown in the inset. Bottom: Spectrum of the reaction product of **1**-OTf with ^{s}PhIO and $Sc(OTf)_3$ (or $^{s}PhI(OAc)_2$) in CH_2Cl_2 at 10 K (frequency 9.63075 GHz; power 0.20 mW; modulation 0.75 mT). Simulation parameters for **3** (60 % yield, –•–•): $D = 10\ \text{cm}^{-1}$, $E/D = 0.15 \pm 0.01$, $\sigma(E/D) = 0.05$, $g_x = 2.33$, $g_y = 2.33$, $g_z = 2.10$, and $A_z = 100 \times 10^{-4}\ \text{cm}^{-1}$; the remaining signal (•••••), which corresponds to 40 % of the total spin, has simulation parameters similar to **1**-OTf.

tensor of $75\times10^{-4}\,\mathrm{cm}^{-1}$. The hyperfine interaction along the x and y directions is small and could not be resolved.

Compound **2** was also found to have an $S=3/2$ ground state with an EPR spectrum strikingly similar to that of **1**-OTf (Supporting Information, Figure S4); the main differences are a slightly higher g_z value of 2.10 and slightly lower A_z value of $70\times10^{-4}\,\mathrm{cm}^{-1}$. The similarity between the EPR spectra of **1**-OTf and **2** point towards closely related electronic structures in the two cases. We propose **2** to have the structure $[(\mathrm{TMG_3tren})\mathrm{Co^{II}OIPh^s}]^{2+}$ that is similar to $[(\mathrm{porphyrin})\mathrm{Fe^{III}OIPh}]^{+}$ reported by Nam et al.,[17] which was found to be in equilibrium with $[(\mathrm{porphyrin})^{+\bullet}\mathrm{Fe^{IV}{=}O}]^{+}$ and PhI [Eq. (1)]. We presume that the cleavage of the I–O bond to generate the desired $\mathrm{Co^{IV}{-}O}$ species [Eq. (2)] is prevented by the high $\mathrm{Co^{II/IV}}$ oxidation potential, which is reflected in only a limited number of known $\mathrm{Co^{IV}}$ complexes.[5,18] EPR spectra of a series of $[(\mathrm{TMG_3tren})\mathrm{Co^{II}X}]^{n+}$ complexes ($X=\mathrm{Cl^-}$, $\mathrm{OTf^-}$, $\mathrm{CH_3CN}$; $n=1$, 2) show that the EPR parameters of $\{\mathrm{Co^{II}}\text{-}(\mathrm{TMG_3tren})\}$ complexes are not highly sensitive to the nature of the fifth ligand, which may also explain the similar EPR spectra of **1**-OTf and **2** (Supporting Information, Figure S4).

$$[(\mathrm{porphyrin})\mathrm{Fe^{III}{-}OIPH}]^{+} \rightleftharpoons [(\mathrm{porphyrin})^{+\bullet}\mathrm{Fe^{IV}{=}O}]^{+} + \mathrm{PhI} \qquad (1)$$

$$[(\mathrm{TMG_3tren})\mathrm{Co^{III}{-}OIPH}]^{2+} \rightleftharpoons [(\mathrm{TMG_3tren})\mathrm{Co^{IV}{-}O}]^{2+} + \mathrm{PhI} \qquad (2)$$

The EPR spectrum of the reaction product of **1**-OTf with ^{s}PhIO and $\mathrm{Sc(OTf)_3}$ exhibits a superposition of an axial spectrum like that of unreacted **1**-OTf (or **2**) and a new rhombic signal with $g_\perp^{\mathrm{eff}}=5.60$ and $g_\parallel^{\mathrm{eff}}=2.10$, which corresponds to 60 % of the total cobalt spin (Figure 2 bottom). This subspectrum, which we assign to the $\{\mathrm{Co^{IV}{-}O{-}Sc^{3+}}\}$ complex **3**, was simulated with a new $S=3/2$ species with $g_\perp=2.33$ and $g_\parallel=2.10$ and marked rhombicity $E/D=0.15\pm0.01$, thus indicative of an asymmetric cobalt center in **3**.[19] The hyperfine coupling along g_z is also remarkably large ($A_z=100\times10^{-4}\,\mathrm{cm}^{-1}$) compared to that of **1**-OTf and **2**. The rhombic distortion reveals significant deviation of the $\{\mathrm{Co^{IV}{-}O{-}Sc^{3+}}\}$ core from axial symmetry, which is presumably due to steric hindrance of the triflate ligands bound to $\mathrm{Sc^{3+}}$.

DFT calculations on $[\mathrm{Co^{IV}(O)L_A}]^{2+}$ (Supporting Information, Figure S5b; $\mathrm{L_A}$ represents the truncated TMG$_3$tren ligand with the end methyl groups replaced by hydrogen atoms) also support the $\mathrm{Co^{IV}}$ (d^5, $S=3/2$) assignment for **3**. The quartet state was calculated to be more stable than the doublet and the sextet states by 13 and $8\,\mathrm{kcal\,mol^{-1}}$, respectively. A quartet ground state was also calculated for the $[\mathrm{Co^{IV}(O)TMG_3tren}]^{2+}$ complex; however, the sextet excited state was found to be only $5\,\mathrm{kcal\,mol^{-1}}$ higher in energy. As no evidence of a low lying excited state was observed in the EPR study, we assume that the $[\mathrm{Co^{IV}(O)L_A}]^{2+}$ complex, where the terminal oxo unit is engaged in extensive H-bonding interactions with the N-bound hydrogen atoms (Supporting Information, Figure S5b), models the $\{\mathrm{Co^{IV}\text{-}O\text{-}Sc}\}^{3+}$ core in **3** better.

The Co K-edge X-ray absorption spectrum (Figure 3 a) of **3** reveals an edge energy of (7720.04 ± 0.2) eV (versus (7718.79 ± 0.1) eV for **1**-OTf and **2**), thereby showing a higher oxidation state of cobalt in **3** as compared to **1**-OTf and **2**. However, the area of the pre-edge peak, which relates to the Co–O covalency,[20] remained unchanged on going from **1**-OTf to **3**. This can be the result of the strong binding of the $\mathrm{Sc^{3+}}$ ion to the $\{\mathrm{CoO}\}^{2+}$ unit, which decreases the π bonding between the cobalt center and the oxo ligand to the extent that there is essentially no multiple-bond character present.

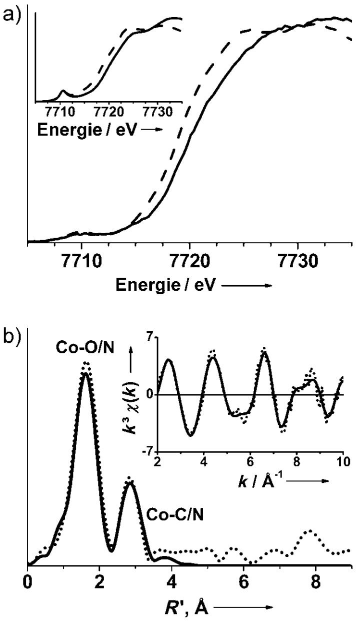

Figure 3. X-ray absorption spectroscopy (XAS) at the cobalt *K* edge. a) XANES spectra of **1**-OTf (-----) and **3** (——); the inset shows the calculated XANES spectra of **1**-OTf and **3** based on structural parameters obtained by the DFT calculations (see also the Supporting Information, Figure S11 and Table S3). b) Fourier-transformed EXAFS spectra of **3**; the inset shows the EXAFS data on a wavevector scale before calculation of the Fourier transform (••••• from experiment, —— simulation). In (a), the spectrum of **3** was corrected for 40 % **1**-OTf (fraction as obtained from EPR analysis). For details, see the Supporting Information.

Direct evidence for a cobalt–oxo unit in **3** is obtained from an analysis of the extended X-ray absorption fine structure (EXAFS) region of the X-ray absorption spectrum (Figure 3 b). The best fit is obtained with an O/N scatterer at 1.85 Å (assigned to the $\{\mathrm{Co^{IV}{-}O}\}$ unit) and a further shell of 4 O/N scatterers at 2.01 Å (corresponding to N donor atoms of the supporting ligand). Fitting was also performed by considering only one shell of 5 O/N scatterers at 1.99 Å; the quality of the fit was significantly improved by incorporating an additional O/N shell (Supporting Information, Table S1). The best fit of the EXAFS of **1**-OTf, in contrast, was obtained with 5 O/N scatterers at 2.05 Å (Supporting Information, Figure S6 and Table S2). To test the authenticity of our EXAFS analysis we also calculated (see Supporting Information) the XANES spectra of **3** (Figure 3 a inset; Supporting Information, Table S3, Figure S11), which could successfully predict the absence of an increase in the pre-edge height and the edge shift of about 1.3 eV on going from **1**-OTf to **3**.

The 1.85 Å distance, assigned to the oxo ligand in EXAFS, closely matches the 1.813(1) Å distance obtained for the isoelectronic $\{\mathrm{Fe^{III}{-}O}\}$ complex^{10} and the DFT-calculated

Co–O distance of 1.81 Å for the $S = 3/2$ $[Co^{IV}(O)L_A]^{2+}$ complex. In contrast, the calculated structure of the corresponding $[Fe^{IV}(O)L_A]^{2+}$ complex (Supporting Information, Figure S5c) gave a much shorter Fe–O distance (1.67 Å) and lacked the H-bonding interactions of the oxo ligand with the N-bound hydrogen atoms of the ligand that are predominant in $[Co^{IV}(O)L_A]^{2+}$. This is consistent with the results of a previous calculation,[21] which predicted a larger spin density on the oxygen of the $\{CoO\}^{2+}$ core compared to that on $\{FeO\}^{2+}$. A significantly shorter Co–O distance of 1.76 Å was calculated for the $[Co^{IV}(O)TMG_3tren]^{2+}$ complex, where H-bonding interactions with the ligand are not possible. Thus, in comparison to the binding of Sc^{3+} to the oxo group of $[(TMC)Fe^{IV}(O)]^{2+}$ that resulted in an elongation of the Fe–O distance by 0.11 Å,[12] the presence of H-bonds in the oxocobalt(IV) complex elongated the Co–O distance by 0.05 Å.

Compound **3** displays the signature reactivity features of an oxidizing metal–oxo complex that is consistent with the $\{Co^{IV}–O–Sc^{3+}\}$ formulation. Thus, reaction of excess triphenylphosphine (50 equiv) with preformed **3** quantitatively produced triphenylphosphine oxide, regenerating **1**-OTf at −30 °C (Supporting Information, Figure S7). A second-order rate constant (k_2) of 0.02 $L\,mol^{-1}\,s^{-1}$ was determined, which is 55 times slower than that reported for the corresponding $[Fe^{IV}(O)(TMG_3tren)]^{2+}$ complex **4**.[9a] Compound **3** was, however, found to be a better one-electron oxidant than **4**. Although **3** reacted efficiently with ferrocene (Fc) and 1,1′-dibromoferrocene [Br_2Fc; $E_{1/2} = 310$ mV versus Fc],[22] generating the corresponding cations and Co^{III} (the resultant solution was EPR silent) in near quantitative yields (Supporting Information, Figure S8), compound **4** could only oxidize Fc and did not react with Br_2Fc.

Complex **3** also reacted with dihydroanthracene (DHA), yielding 60 % **1**-OTf (Supporting Information, Figure S9).[23] The organic products of the reaction were anthracene (An) and anthraquinone (AnQ), in respective yields of 27 % and 45 %, which account for 2.07 oxidizing equivalents of ^{s}PhIO (out of 3 equiv). In contrast, no AnQ was formed during reaction of **4** with DHA; only An was generated in 50 % yield.[9a] The six-electron oxidation of An to AnQ, which was also observed previously with other high-potential metal–oxo complexes,[24] is probably initiated by a rapid electron transfer from An to **3** to produce the radical cation ($An^{+\bullet}$).[25] This result again reflects the stronger one-electron oxidizing properties of **3** than **4**.

The reactivity of **2** was also investigated and compared with that of **3** (Supporting Information, Table S4). While **2** performed oxo transfer to PPh_3 at a rate comparable to that of **3**, it was found to be more efficient in its H-atom abstracting ability from DHA.[26] Anthracene and anthraquinone were obtained in higher yields of 40 % and 65 %, respectively, which correspond to all oxidizing equivalents of ^{s}PhIO. However, **2** was found to be a sluggish oxidant in its reaction with Fc and Br_2Fc; the corresponding cations were formed in only 20 % and 10 % yields, respectively (Supporting Information, Figure S8 and Table S4).

In summary, we have isolated and characterized a $[Co^{IV}(O)(TMG_3tren)]^{2+}$ complex **3**, which is the first example of a coordination complex having a $\{Co^{IV}–O\}$ unit in an $S = 3/2$ configuration. The small number of previously characterized Co^{IV} complexes[5,18] all occur in a low-spin $S = 1/2$ state. The isoelectronic $\{Fe^{III}–O\}$ complex,[10] in contrast, possessed an $S = 5/2$ state. The quartet ground state of **3** is consistent with the results of the previous[21] and present DFT calculations on $\{Co^{IV}–O\}$ complexes of closely related ligands. The highly reactive $\{Co^{IV}–O\}$ unit in **3** is stabilized by its Lewis acid interaction with Sc^{3+} ions, thereby generating a $\{Co^{IV}–O–Sc^{3+}\}$ core. In the absence of Sc^{3+}, the Co^{IV} oxidation state was not accessible, and the reaction of **1**-OTf with ^{s}PhIO only yielded the cobalt(II)–iodosylbenzene adduct **2**. The reactivities of **2** and **3** compared to each other and to that of the corresponding oxoiron(IV) complex **4** showed different trends with respect to electron transfer from 1,1′-dibromoferrocene, H-atom abstraction from DHA, and oxo transfer to PPh_3. The electron-transfer ability of the complexes was found to decrease in the order $\mathbf{3} \gg \mathbf{2} > \mathbf{4}$. For the H-atom abstraction reaction, a different reactivity order, $\mathbf{2} > \mathbf{3} > \mathbf{4}$, was observed. The oxo transfer abilities of **2** and **3** were, however, found to be comparable to each other, and much lower than that for **4**. Stronger one-electron oxidizing and H-atom abstraction but weaker oxo-transfer capabilities of **2** and **3** compared to **4** may originate from the higher oxyl radical character of the $\{CoO\}^{2+}$ unit compared to $\{FeO\}^{2+}$. Detailed DFT calculations to better understand the reactivity trends in **2**, **3**, and **4** are in progress. The present results set the stage for future efforts aimed at more efficient oxidation reactions carried out by cobalt as well as other elusive transition metal oxo complexes using the stabilizing interactions of redox-inactive metal ions such as Sc^{3+} and Ca^{2+}.

Received: September 18, 2010

Keywords: bioinorganic chemistry · cobalt · Lewis acid interactions · scandium · terminal coordination

---

[1] a) J. W. Egan, Jr., B. S. Haggerty, A. L. Rheingold, S. C. Sendlinger, K. H. Theopold, *J. Am. Chem. Soc.* **1990**, *112*, 2445 – 2446; b) O. M. Reinaud, K. H. Theopold, *J. Am. Chem. Soc.* **1994**, *116*, 6979 – 6980; c) W. Nam, I. Kim, Y. Kim, C. Kim, *Chem. Commun.* **2001**, *14*, 1262 – 1263.

[2] C. J. Chang, Z.-H. Loh, C. Shi, F. C. Anson, D. G. Nocera, *J. Am. Chem. Soc.* **2004**, *126*, 10013 – 10020.

[3] a) M. Schlangen, H. Schwarz, *Chem. Commun.* **2010**, *46*, 1878 – 1880; b) I. F. Taylor, S. J. Blanksby, S. B. Colbran, G. D. Willett, *Rapid Commun. Mass Spectrom.* **2010**, *24*, 1142 – 1146.

[4] a) B. S. Brunschwig, M. H. Chou, C. Creutz, P. Ghosh, N. Sutin, *J. Am. Chem. Soc.* **1983**, *105*, 4832 – 4833; b) M. W. Kanan, Y. Surendranath, D. G. Nocera, *Chem. Soc. Rev.* **2009**, *38*, 109 – 114; c) J. G. McAlpin, Y. Surendranath, M. Dincă, T. A. Stich, S. A. Stoian, W. H. Casey, D. G. Nocera, R. D. Britt, *J. Am. Chem. Soc.* **2010**, *132*, 6882 – 6883; d) M. W. Kanan, J. Yano, Y. Surendranath, M. Dincă, V. K. Yachandra, D. G. Nocera, *J. Am. Chem. Soc.* **2010**, *132*, 13692 – 13701; e) M. Risch, V. Khare, I. Zaharieva, L. Gerencser, P. Chernev, H. Dau, *J. Am. Chem. Soc.* **2009**, *131*, 6936 – 6937.

[5] a) J. K. Beattie, C. U. Beck, P. A. Lay, A. F. Masters, *Inorg. Chem.* **2003**, *42*, 8366 – 8370; b) K. Dimitrou, A. D. Brown, T. E. Concolino, A. L. Rheingold, G. Christou, *Chem. Commun.* **2001**,

1284 – 1285; c) A. C. Masset, C. Michel, A. Maignan, M. Hervieu, O. Toulemonde, F. Studer, B. Raveau, J. Hejtmanek, *Phys. Rev. B* **2000**, *62*, 166 – 175.

[6] C. Limberg, *Angew. Chem.* **2009**, *121*, 2305 – 2308; *Angew. Chem. Int. Ed.* **2009**, *48*, 2270 – 2273.

[7] H. Wittmann, V. Raab, A. Schorm, J. Plackmeyer, J. Sundermeyer, *Eur. J. Inorg. Chem.* **2001**, 1937 – 1948.

[8] C. Würtele, E. Gaoutchenova, K. Harms, M. C. Holthausen, J. Sundermeyer, S. Schindler, *Angew. Chem.* **2006**, *118*, 3951 – 3954; *Angew. Chem. Int. Ed.* **2006**, *45*, 3867 – 3869.

[9] a) J. England, M. Martinho, E. R. Farquhar, J. R. Frisch, E. L. Bominaar, E. Münck, L. Que, Jr., *Angew. Chem.* **2009**, *121*, 3676 – 3680; *Angew. Chem. Int. Ed.* **2009**, *48*, 3622 – 3626; b) J. England, Y. Guo, E. R. Farquhar, V. G. Young, Jr., E. Münck, L. Que, Jr., *J. Am. Chem. Soc.* **2010**, *132*, 8635 – 8644.

[10] C. E. MacBeth, A. P. Golombek, V. G. Young, Jr., C. Yang, K. Kuczera, M. P. Hendrich, A. S. Borovik, *Science* **2000**, *289*, 938 – 941.

[11] a) M. Yagi, M. Kaneko, *Chem. Rev.* **2001**, *101*, 21 – 36; b) J. P. McEvoy, G. W. Brudvig, *Chem. Rev.* **2006**, *106*, 4455 – 4483; c) J. Yano, J. Kern, K. Sauer, M. J. Latimer, Y. Pushkar, J. Biesiadka, B. Loll, W. Saenger, J. Messinger, A. Zouni, V. K. Yachandra, *Science* **2006**, *314*, 821 – 825; d) H. Dau, C. Limberg, T. Reier, M. Risch, S. Roggan, P. Strasser, *ChemCatChem* **2010**, *2*, 724 – 761.

[12] S. Fukuzumi, Y. Morimoto, H. Kotani, P. Naumov, Y.-M. Lee, W. Nam, *Nat. Chem.* **2010**, *2*, 756 – 759.

[13] A. W. Addison, T. N. Rao, J. Reedijk, J. Rijn, G. C. Verschoor, *J. Chem. Soc. Dalton Trans.* **1984**, 1349 – 1356.

[14] D. Macikenas, E. Skrzypczak-Jankun, D. J. Protasiewicz, *J. Am. Chem. Soc.* **1999**, *121*, 7164 – 7165.

[15] No spectral changes were observed in control reactions in which **1**-OTf was made to react with $Sc(OTf)_3$ or $^{s}PhI(OAc)_2$ in the absence of $^{s}PhIO$.

[16] C. Benelli, D. Gatteschi, *Inorg. Chem.* **1982**, *21*, 1788 – 1790.

[17] W. Nam, S. K. Choi, M. H. Lim, J.-U. Rohde, I. Kim, J. Kim, C. Kim, L. Que, Jr., *Angew. Chem.* **2003**, *115*, 113 – 115; *Angew. Chem. Int. Ed.* **2003**, *42*, 109 – 111.

[18] a) S. Will, J. Lex, E. Vogel, V. A. Adamian, E. V. Caemelbecke, K. M. Kadish, *Inorg. Chem.* **1996**, *35*, 5577 – 5583; b) J. Harmer, S. V. Doorslaer, I. Gromov, M. Bröring, G. Jeschke, A. Schweiger, *J. Phys. Chem. B* **2002**, *106*, 2801 – 2811; c) S. Fukuzumi, K. Miyamoto, T. Suenobu, E. V. Caemelbecke, K. M. Kadish, *J. Am. Chem. Soc.* **1998**, *120*, 2880 – 2889; d) T. J. Collins, R. D. Powell, C. Slebodnick, E. S. Uffelman, *J. Am. Chem. Soc.* **1991**, *113*, 8419 – 8425; e) G. C. Alley, K. D. Warren, *Inorg. Chem.* **1969**, *8*, 1902 – 1904; f) T. Goslinski, C. Zhong, M. J. Fuchter, C. L. Stern, A. J. P. White, A. G. M. Barrett, B. M. Hoffman, *Inorg. Chem.* **2006**, *45*, 3686 – 3694; g) F. C. Anson, T. J. Collins, R. J. Coots, S. L. Gipson, T. G. Richmond, *J. Am. Chem. Soc.* **1984**, *106*, 5037 – 5038.

[19] The D value was not determined because of the missing traces from the "$m_s = \pm 3/2$" doublet.

[20] R. K. Hocking, S. D. George, K. N. Raymond, K. O. Hodgson, B. Hedman, E. I. Solomon, *J. Am. Chem. Soc.* **2010**, *132*, 4006 – 4015.

[21] C. Michel, E. J. Baerends, *Inorg. Chem.* **2009**, *48*, 3628 – 3638.

[22] T. Nakanishi, K. Ohkubo, T. Kojima, S. Fukuzumi, *J. Am. Chem. Soc.* **2009**, *131*, 577 – 584.

[23] k_2 could not be determined for this reaction owing to the absence of pseudo first-order behavior, which is probably due to the presence of the excess $^{s}PhIO$ (3 equiv) that was necessary to synthesize **3**.

[24] a) A. S. Larsen, K. Wang, M. A. Lockwood, G. L. Rice, T.-J. Won, S. Lovell, M. Sadílek, F. Tureček, J. M. Mayer, *J. Am. Chem. Soc.* **2002**, *124*, 10112 – 10123; b) S. P. Visser, K. Oh, A.-R. Han, W. Nam, *Inorg. Chem.* **2007**, *46*, 4632 – 4641.

[25] S. Fukuzumi, I. Nakanishi, K. Tanaka, *J. Phys. Chem. A* **1999**, *103*, 11212 – 11220.

[26] **1**-OTf was regenerated during reaction of **2** with DHA or PPh_3.